A Discrete Element Method Approach to Progressive Localization of Fractures and Associated Seismicity: Applications to Sandstone, Marble and Granite

Harsha Vora (hv6@rice.edu), Julia Morgan (morganj@rice.edu)

Department of Earth, Environmental and Planetary Sciences, Rice University, Houston, TX

Objective

The objective of our study is to understand the growth and coalescence of fractures, and associated fracture energy, in sandstone, marble and granite. We conduct a quantitative analysis of the temporal and spatial growth of microfractures, and their associated modes, during confined biaxial experiments simulated using the Discrete Element Method. We employ the calculations of fracture energy, seismic b-value, fractal D-value to interpret the distinct microfracturing patterns in soft and hard rocks and the effect of confining pressure. We present a scale independent relationship between the seismic b-value and fractal D-value.

The Discrete Element Method

- Construct geologic medium as assemblage of simple particles – disks or spheres
- Apply physical properties to particles: Contact friction, elastic properties.
- Interparticle bonds to simulate cohesion, which can fail under normal, shear, and rotational stresses
- Resolve forces onto particles and track resultant motion

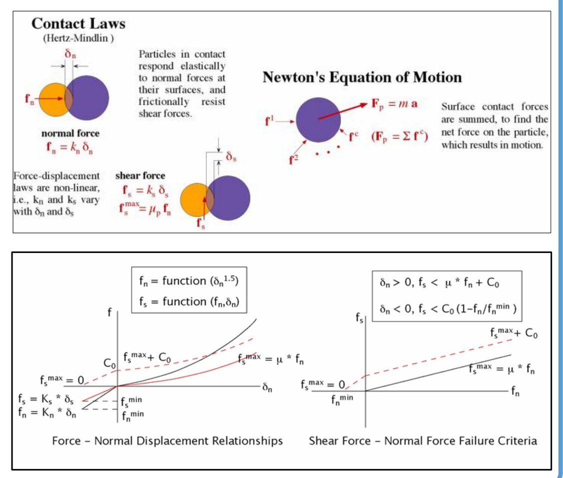

Discrete Element Model Setup and Analysis

1. **Setup biaxial experimental setup**
   - Domain size: 0.12m x 0.06 m
   - 2700 particles with radius of 400 µm
     3240 particles with radius of 300 µm
   - Preconsolidate each sample to 10 MPa

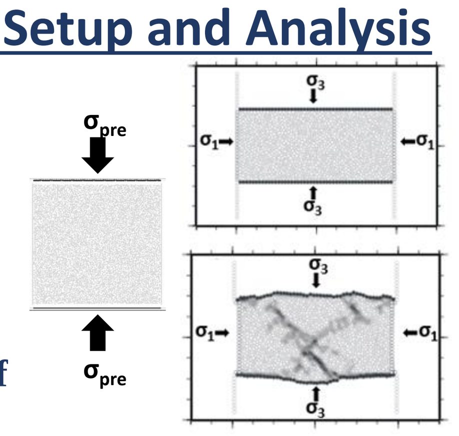

2. **Calibrate bulk physical properties of simulated samples to rock types**

Rock Type	Youngs Modulus of Bonds (GPa)	Shear Modulus of Bonds (GPa)	Tensile Strength of Bonds (MPa)	Cohesion of Bonds (MPa)	Shear Modulus of Particles (GPa)	Interparticle friction	Poissons Ratio of Particles
Berea Sandstone	5	5	75	75	29	0.40	0.33
Carrara Marble	10	10	200	400	2000	0.50	0.38
Lac du Bonnet Granite	50	50	533	800	2000	0.70	0.26

Rock Type	Unconfined Compressive Strength (MPa)	Bulk Youngs Modulus (GPa)	Mohr-Coulomb Cohesion (MPa)	Mohr-Coulomb Slope	Angle of Friction (Degrees)
Berea Sandstone	94.52	5.10	28.00	0.51	26.83
Carrara Marble	104.85	24.18	34.27	0.67	33.90
Lac du Bonnet Granite	207.83	40.84	49.90	0.93	43.01

3. **Conduct biaxial compression experiments** on simulated rocks at confining pressures of 0, 2, 5, 10, 20, 30, 40 and 50 MPa.
4. **Calculate energy and moment of Acoustic Emissions associated with microfractures**

$$E_f = \left(\frac{1}{2C_f}\right)\sigma_{cf}^2 v_f$$

$$M_e = \frac{2}{3}log_{10}E_f - 2.9$$

E_f : energy of micro-fracture
C_f :Modulus of failed element – Youngs or Shear
σ_{cf} : Peak strength of element
v_f : Volume of failed element
M_e : Moment

5. **Evaluate fractal nature of microfracturing using D-value**

$$C(R) = \frac{2}{N(N-1)} N_{(r<R)}$$

$$C(R) \; \alpha \; R^{\boldsymbol{D}}$$

D: fractal dimension
N: number of microfracture event pairs
R: radius (m)

Low D-value: Localized Damage
High D-value: Distributed Damage

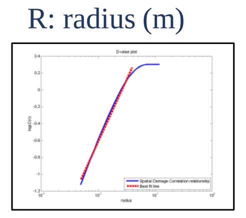

6. **Spatial and Temporal Clustering of Microfractures**
   - D-value of clusters is maintained equal to original D-value of microfractures
   - Spatial limit: 0.0012 m
   - Temporal limit: 0.001 strain

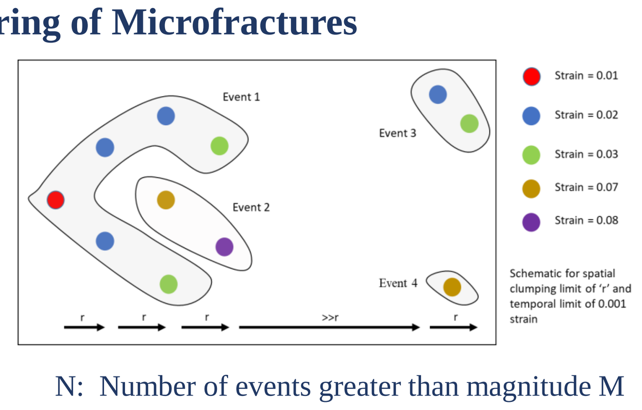

7. **Calculate b-value**

$$log\, N(M) = a - \boldsymbol{b}M$$

N: Number of events greater than magnitude M
b: slope of frequency-magnitude

Growth of Fractures: Microfracture Patterns, Energy and b-value

Confining = 0 MPa

Berea Sandstone

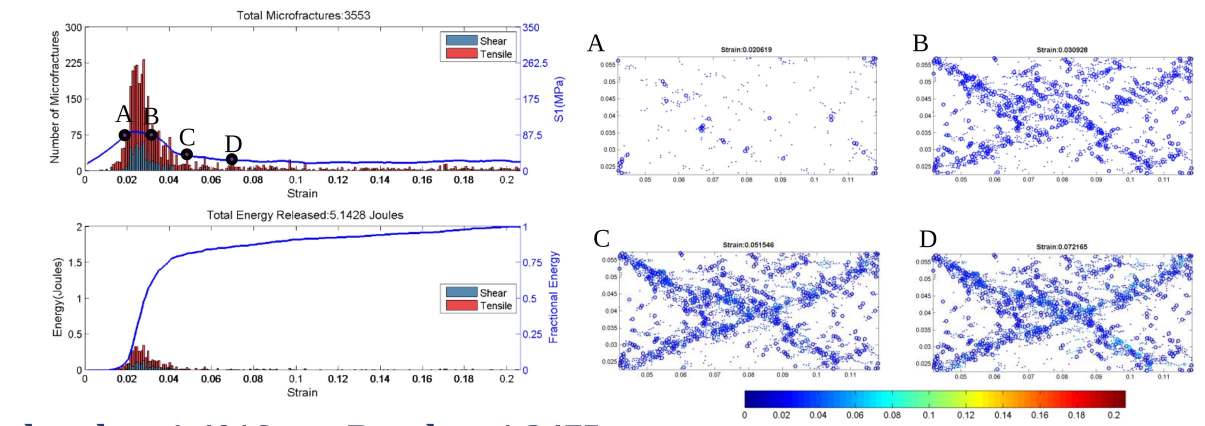

b-value: 1.4016 D-value: 1.2475

. = tensile failure Strain **o** = shear failure

Carrara Marble

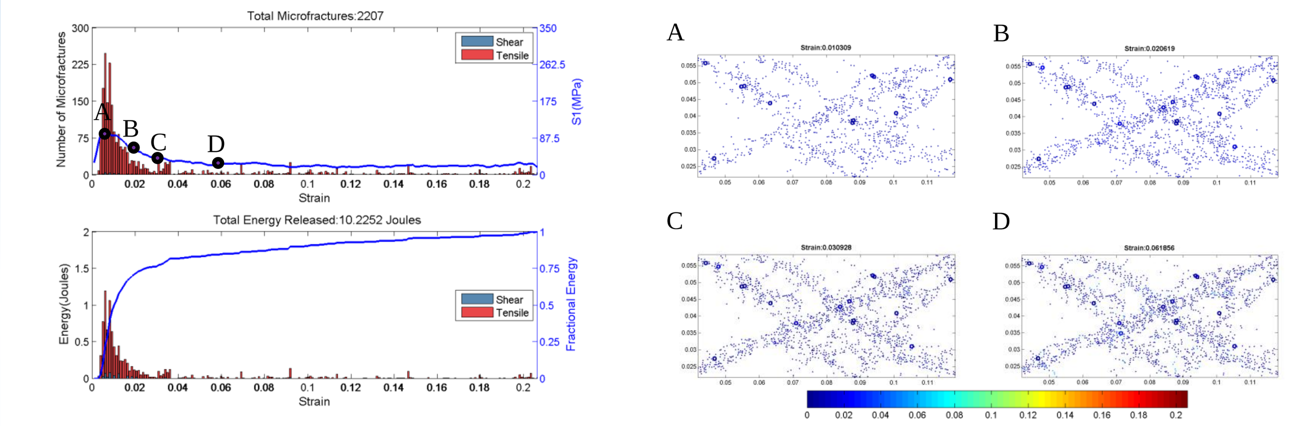

b-value: 1.4400 D-value: 1.2251

. = tensile failure Strain **o** = shear failure

Lac du Bonnet Granite

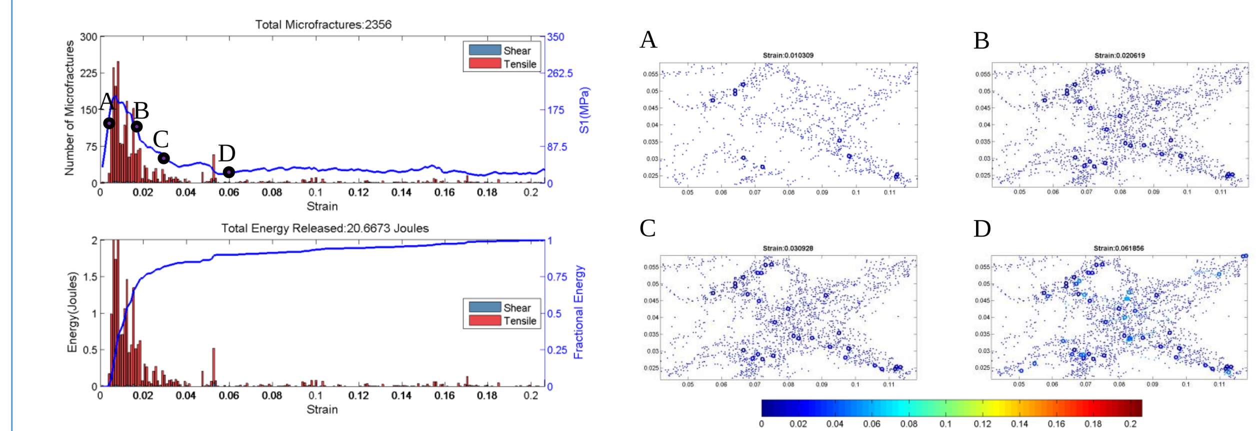

b-value: 1.4764 D-value: 1.1991

. = tensile failure Strain **o** = shear failure

Confining = 10 MPa

Berea Sandstone

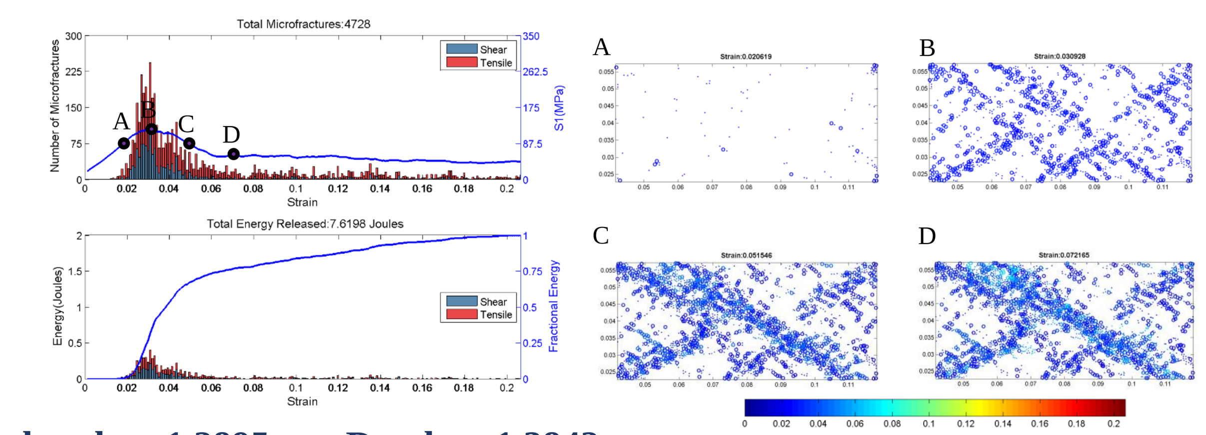

b-value: 1.2895 D-value: 1.3842

. = tensile failure Strain **o** = shear failure

Carrara Marble

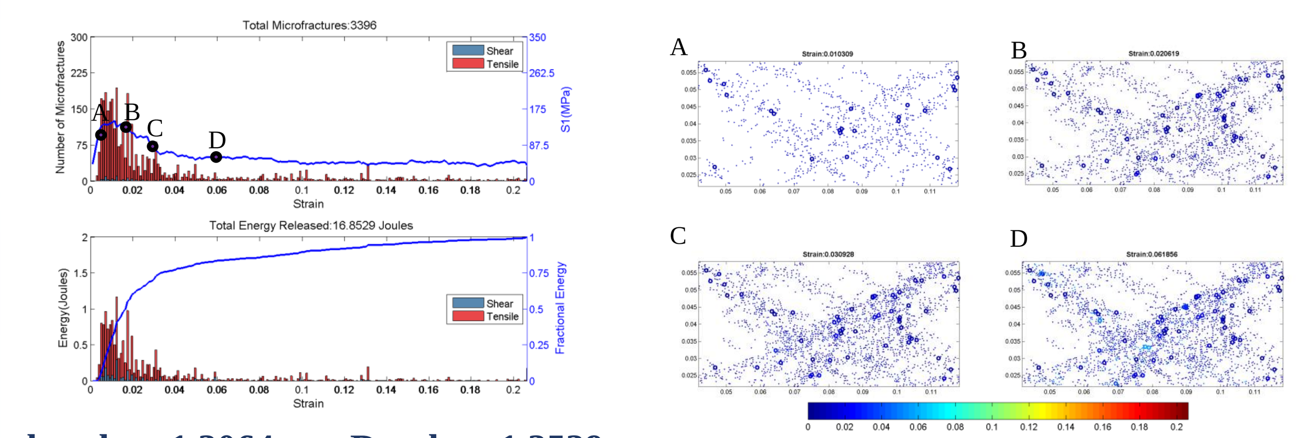

b-value: 1.3064 D-value: 1.3539

. = tensile failure Strain **o** = shear failure

Lac du Bonnet Granite

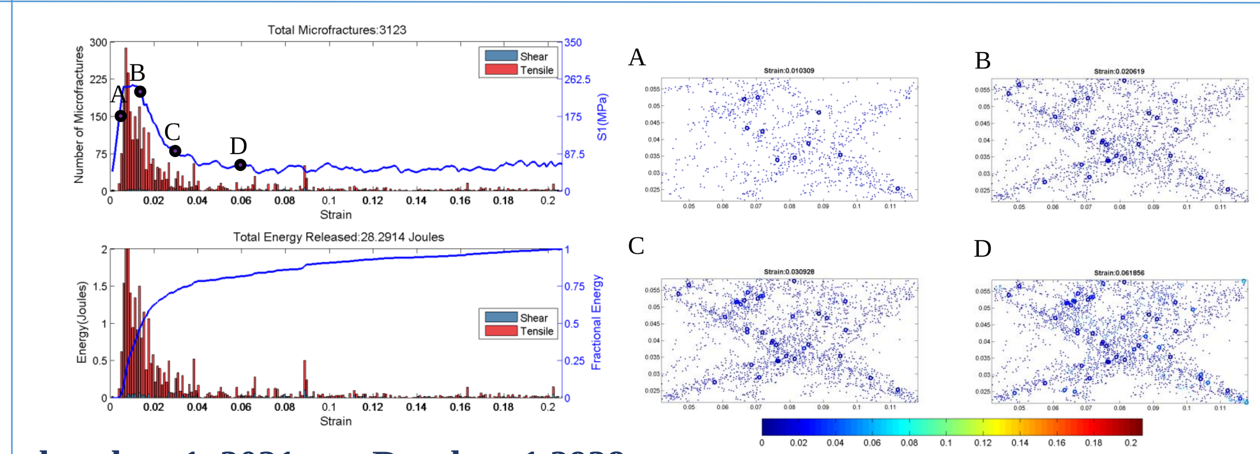

b-value: 1. 3021 D-value: 1.2938

. = tensile failure Strain **o** = shear failure

Confining = 30 MPa

Berea Sandstone

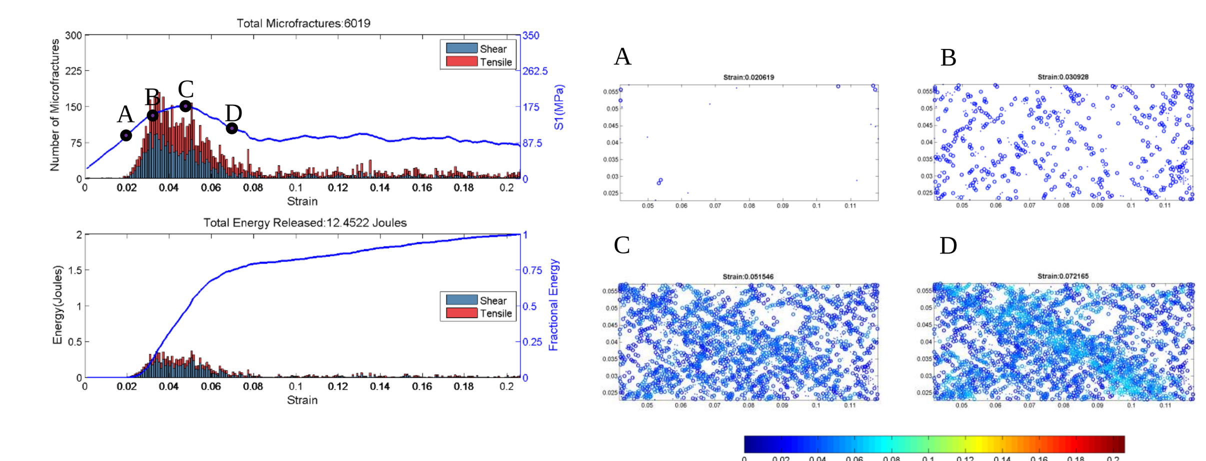

b-value: 1.1036 D-value: 1.4716

. = tensile failure Strain **o** = shear failure

Carrara Marble

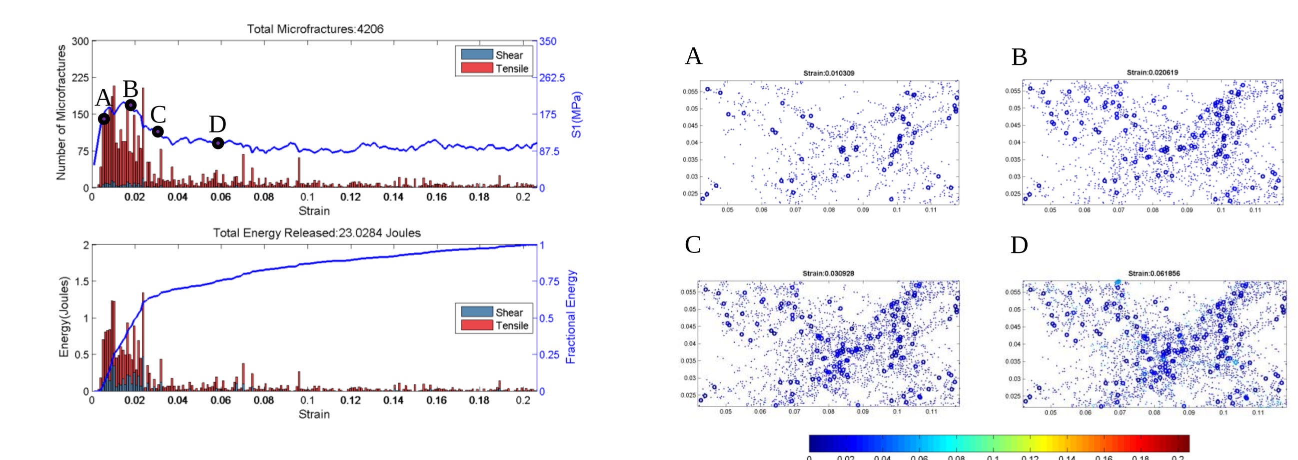

b-value: 1.1534 D-value: 1.4533

. = tensile failure Strain **o** = shear failure

Lac du Bonnet Granite

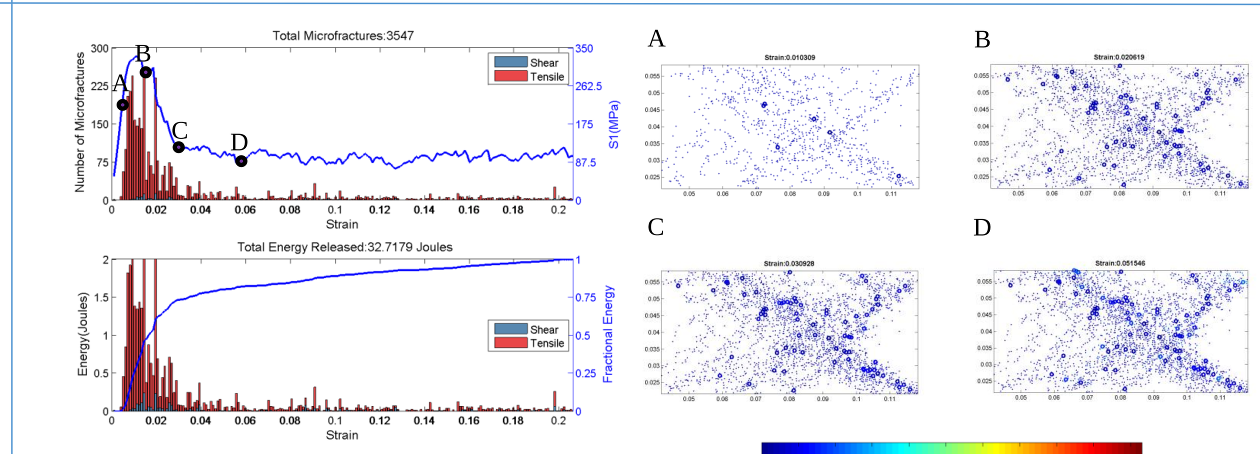

b-value: 1.1898 D-value: 1.4180

. = tensile failure Strain **o** = shear failure

Effect of Confining Pressure on Microfracturing and Energy

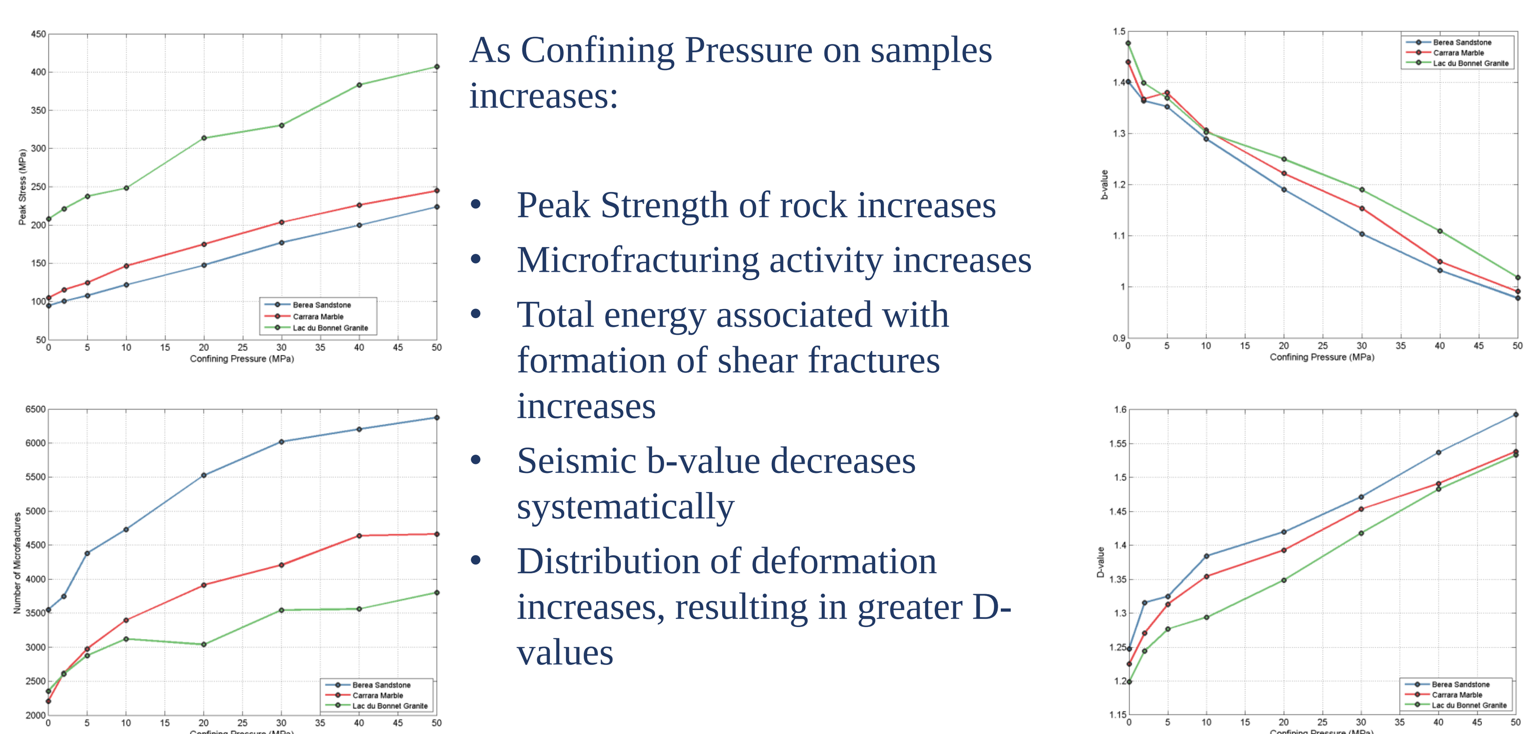

As Confining Pressure on samples increases:

- Peak Strength of rock increases
- Microfracturing activity increases
- Total energy associated with formation of shear fractures increases
- Seismic b-value decreases systematically
- Distribution of deformation increases, resulting in greater D-values

Seismic b-values and Fractal D-values exhibit a scale-independent linear relationship, indicating similarity between microfracturing and fault processes associated with earthquakes.

$$D = -0.72 * b + 2.27$$

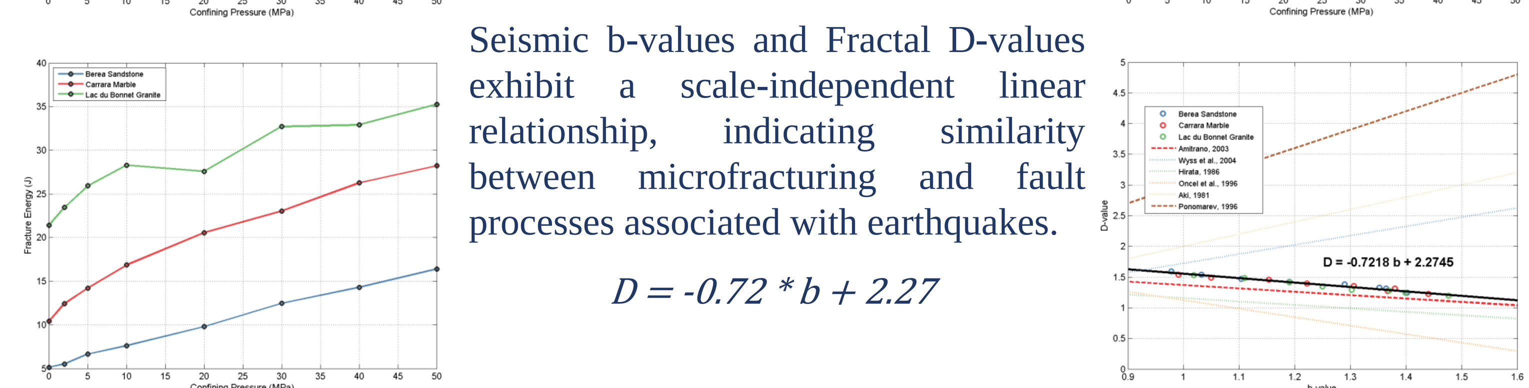

Effect of Rock Type on Microfracturing

As strength of the rock increases, the tendency of microfractures occurring in shear mode decreases.

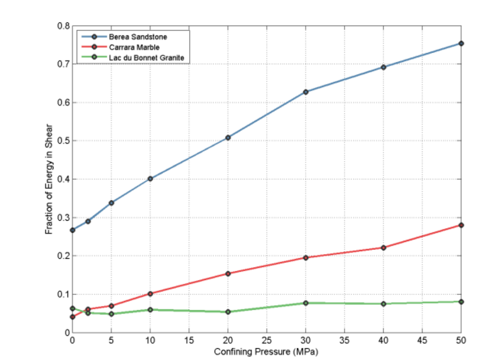

We interpret that fracture growth is observed occurs through coalescence of asperities formed under shear through extensional microfractures in weaker rocks such as sandstones.

For stronger rocks, rupture growth and propagation is dominated by coalescence of extensional microfractures.

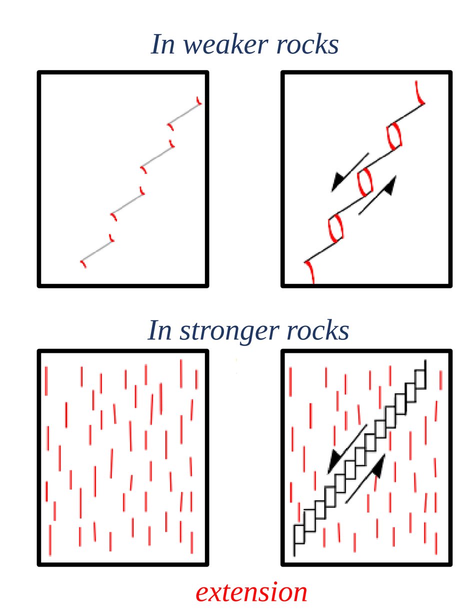

Future Work: To study the orientation of induced microfractures in sandstone, marble and granite to test the validity of our interpretation.

Conclusions

1. Micromechanical observations suggest that nucleation, growth and interaction of microcracks are the dominant, controlling microevents which lead to macroscopic fracture and failure of rocks under compression.
2. In weaker rocks such as the Berea Sandstone:
   - Through-going fracture is formed by extensional microfractures that propagate from flaws loaded under shear.
   - Growth of shear microfractures increases with confining pressure.
3. In stronger rocks such as the Lac du Bonnet Granite
   - Growth of through-going occurs through the coalescence of extensional fractures.
   - Shearing does not play a dominant role in development of fractures
4. As confining pressure on rock increases:
   - Number of microfractures and their distribution increases.
   - Seismic b-value decreases.
   - Peak stress and energy for fracture genesis and coalescence increases.
5. Seismic b-values and fractal D-values exhibit a scale-independent linear relationship upon brittle deformation.

References

- Lockner, D. (1993), The role of acoustic emission in the study of rock fracture, *Int. J. Rock Mech. Min. Sci. Geomech. Abstr.*, *30*(7), 883–899, doi:10.1016/0148-9062(93)90041-B.
- Tang, C. ., and P. . Kaiser (1998), Numerical Simulation of Cumulative Damage and Seismic Energy Release During Brittle Rock Failure—Part I: Fundamentals, *Int. J. Rock Mech. Min. Sci.*, *35*(2), 113–121, doi:10.1016/S0148-9062(97)00009-0.
- Morgan, J. K. (1999), Numerical simulations of granular shear zones using the distinct element method 2 . Effects of particle size distribution and interparticle, *J. Geophys. Res.*, *104*(B2), 2721–2732.
- Hazzard, J. F., R. P. Young, and S. C. Maxwell (2000), Micromechanical modeling of cracking and failure in brittle rocks, *J. Geophys. Res. Solid Earth*, *105*(B7), 16683–16697, doi:10.1029/2000JB900085.
- Wang, B., Y. Chen, and T. F. Wong (2008), A discrete element model for the development of compaction localization in granular rock, *J. Geophys. Res. Solid Earth*, *113*(3), 1–17, doi:10.1029/2006JB004501.
- Amitrano, D. (2003), Brittle-ductile transition and associated seismicity : Experimental and numerical studies and relationship with the b value, , *108*, 1–15, doi:10.1029/2001JB000680.
- Blenkinsop, T. G. (2008), Relationships between faults , extension fractures and veins , and stress, , *30*, 622–632, doi:10.1016/j.jsg.2008.01.008.